Available online at www.sciencedirect.com
ScienceDirect
European Polymer Journal 43 (2007) 2913–2921
EUROPEAN POLYMER JOURNAL
www.elsevier.com/locate/europolj

Preparation of homogeneous polyacrylamide hydrogels by free-radical crosslinking copolymerization

Esra Arzu Kuru, Nermin Orakdogen, Oguz Okay *

Istanbul Technical University, Department of Chemistry, 34469 Maslak, Istanbul, Turkey

Received 8 March 2007; received in revised form 3 April 2007; accepted 15 April 2007
Available online 27 April 2007

Abstract

Network microstructures of acrylamide (AAm)-based hydrogels were investigated by static and dynamic light scattering techniques. The hydrogels were prepared by free-radical crosslinking copolymerization of the monomers acrylamide (AAm), *N*,*N*-dimethylacrylamide (DMA) and *N*-isopropylacrylamide (NIPA) with *N*,*N*′-methylenebis(acrylamide) as a crosslinker in aqueous solutions. It was observed that the addition of DMA or NIPA into the comonomer feed suppresses the extent of frozen concentration fluctuations in polyacrylamide (PAAm) hydrogels. The cooperative diffusion coefficient increases while both the static and dynamic correlation lengths decrease as the amount of DMA in the comonomer feed is increased. Formation of homogeneous PAAm hydrogels by introduction of hydrophobic moieties was explained as a result of the steric effect of the bulky side groups on DMA or NIPA segments.

Keywords: Hydrogels; Inhomogeneity; Light scattering; Polyacrylamide

1. Introduction

Hydrophilic gels called hydrogels are hydrophilic polymer networks swollen in water. They are able to absorb 10–1000 times their dry volume of water without dissolving. Water inside the hydrogel allows free diffusion of some solute molecules, while the polymer serves as a matrix to hold water together. Hydrogels are mainly prepared by free-radical crosslinking copolymerization (FCC) of acrylamide (AAm)-based monomers with a divinyl monomer (crosslinker) in aqueous solutions. As is well-known, gelation during FCC occurs non-randomly due to the existence of various non-idealities such as the conversion and structure dependent reactivities of the functional groups, cyclization and multiple crosslinking reactions [1,2]. These non-idealities during gelation necessarily result in the formation of hydrogels with a large number of network defects, affecting their physical properties such as swelling, elasticity, transparency, and permeability. One of the network defects is the inhomogeneous distribution of the crosslink points along the gel sample, which is known as the spatial gel inhomogeneity [3,4]. Since the gel inhomogeneity is closely

* Corresponding author. Tel.: +90 212 2853156; fax: +90 212 2856386.
E-mail address: okayo@itu.edu.tr (O. Okay).

0014-3057/$ - see front matter © 2007 Elsevier Ltd. All rights reserved.
doi:10.1016/j.eurpolymj.2007.04.019

connected to the spatial concentration fluctuations, scattering methods have been employed to investigate the spatial inhomogeneities [5–10]. The gel inhomogeneity can be manifested by comparing the scattering intensities from the gel and from a semidilute solution of the same polymer at the same concentration. The scattering intensity from gels is always larger than that from the polymer solution. The excess scattering over the scattering from polymer solution is related to the degree of the inhomogeneities in gels.

Spatial gel inhomogeneity is undesirable for applications because structural inhomogeneity results in a dramatic reduction in the strength of the crosslinked materials. Although the inhomogeneity control in gels is quite sophisticated, the ionization of polymer hydrogels is one of the methods used to suppress the inhomogeneities [3,4,11–15]. Moreover, reducing the crosslinker concentration used in the hydrogel preparation also reduces the degree of spatial gel inhomogeneity [16–19]. Recently, we have shown that the spatial gel inhomogeneity can be controlled by varying the gel point with respect to the critical overlap concentration during the gel preparation stage [20].

Here, we propose a new method to obtain homogeneous AAm-based hydrogels. As will be seen below, the introduction of a hydrophobically modified hydrophilic monomer into the polyacrylamide (PAAm) network chains significantly reduces the inhomogeneity of the resulting hydrogels. The hydrogels were prepared by FCC of the monomer AAm and the crosslinker *N*,*N*′-methylenebis(acrylamide) (BAAm) in aqueous solutions. *N*,*N*-dimethylacrylamide (DMA) and *N*-isopropylacrylamide (NIPA) were used as the hydrophobically modified monomers at various mole ratios. The scattered light intensity profiles during gelation were obtained by real-time light scattering measurements. The microstructure of the resulting hydrogels was characterized by static and dynamic light scattering methods. By the static light scattering method, scattering intensities from the hydrogels were measured at various scattering angles. An equivalent semidilute solution of the copolymers based on AAm/DMA or AAm/NIPA monomers served as a reference in the understanding of the inhomogeneities in gels. Dynamics of the hydrogels were also systematically investigated by dynamic light scattering (DLS) measurements as a function of the hydrophobic group content of the network.

2. Experimental

2.1. Materials

Acrylamide (AAm, Merck), *N*,*N*-dimethylacrylamide (DMA, Fluka), *N*-isopropylacrylamide (NIPA, Aldrich), *N*,*N*′-methylenebis(acrylamide) (BAAm, Merck), ammonium persulfate (APS, Merck), and *N*,*N*,*N*′,*N*′-tetramethylethylenediamine (TEMED) were used as received. Distilled and deionized water (HPLC-grade) was used throughout this study. The stock solutions in water were prepared using the following concentrations: AAm (2.50 g/10 ml), DMA (2.60 ml/10 ml), NIPA (2.45 g/10 ml), BAAm (0.127 g/10 ml), APS (0.080 g/10 ml), and TEMED (0.25 ml/10 ml).

2.2. Hydrogel preparation

The hydrogels were prepared in aqueous solutions at 21 °C in the presence of 3.51 mM APS initiator and 0.25 v/v% TEMED accelerator. The crosslinker ratio, that is the mole ratio of the crosslinker BAAm to the monomers AAm + DMA or AAm + NIPA was fixed at 1/83. The initial concentration of the monomers was also fixed at 5 w/v%. The composition of the comonomer mixture denoted by the mole percent of DMA or NIPA was varied over a wide range. The reactions were carried out in glass tubes as well as in the light scattering vials. To illustrate the synthetic procedure in glass tubes, we give details for the preparation of a PAAm hydrogel with 20 mol% DMA: Stock solutions of AAm (1.45 ml), DMA (0.505 ml), BAAm (0.93 ml), TEMED (1.00 ml), and water (5.12 ml) were mixed in a 10 ml graduated flask. After bubbling nitrogen for 15 min, APS stock solution (1.00 ml) was added to the mixture to give a total volume of 10 ml. The solution was then poured into several glass tubes of 4–5 mm internal diameters and about 100 mm long. The glass tubes were sealed, and the polymerization was conducted at 21 °C for 24 h. The gel samples thus obtained were subjected to the mechanical tests, as will be described below.

For the light scattering measurements, the reactions were also carried out in the light scattering vials. All glassware was kept dustfree by rinsing in hot acetone prior using. The reaction solutions, prepared as described above, were filtered through membrane filters (pore size = 0.2 μm) directly into

the vials in a dustfree glovebox. For the calculation of excess scattering from gels, all the crosslinking polymerizations were repeated under the same experimental conditions except that the crosslinker BAAm was not used.

2.3. Light scattering measurements

Static light scattering measurements were carried out at 21 °C using a commercial multi-angle light scattering DAWN EOS (Wyatt Technologies Corporation) equipped with a vertically polarized 30mW Gallium-arsenide laser operating at $\lambda = 690$ nm and 18 simultaneously detected scattering angles. The light scattering system was calibrated against a toluene standard (Rayleigh ratio at 690 nm $= 9.78 \times 10^{-6}$ cm^{-1}, DAWN EOS software). The scattered light intensities were recorded from angles $\theta = 14.5°$ to 163.3° which correspond to the scattering vector q range 3.1×10^{-4}–2.4×10^{-3} Å^{-1}, where $q = (4\pi n/\lambda)\sin(\theta/2)$, n is the refractive index of the medium.

Dynamic light scattering measurements were performed at 25 °C after a reaction time of 24 h using ALV/CGS-3 compact goniometer (ALV, Langen, Germany) equipped with a cuvette rotation/translation unit (CRTU) and a He–Ne laser (22 mW, wavelength λ of 632.8 nm). The scattering angle was fixed to be 90°. A fiber optical detection unit based on three-mode detection was used, which includes an appropriate collimator/GRIN-lens fiber and the ALV/STATIC and DYNAMIC enhancer. To protect the detector, the intensity of the incident light is automatically attenuated at each measurement by an eight-step automatic software-controlled attenuator and measured with a monitor diode. Thus, the intensity of incident light can be different within a series of measurements. When discussing scattering intensities, we therefore use data that were rescaled to a preset value of the monitor diode assuming a linear count rate dependence. Toluene was used as the index matching liquid. The temperature was controlled with an external thermostat. The time averaged ICFs were acquired at 100 different sample positions selected by randomly moving the CRTU before each run. The acquisition time for each run was 30 s. The ensemble-averaged scattering intensity, $\langle I \rangle_E$, was determined by continuously moving the sample vial with the CRTU, and the acquisition time for $\langle I \rangle_E$ was 3 min.

2.4. Mechanical measurements

All the mechanical measurements were conducted in a thermostated room of 21 ± 0.5 °C. Uniaxial compression measurements were performed on gel samples prepared in glass tubes after a reaction time of 24 h. For this purpose, the gels in the form of rods of about 4 mm in diameter were cut into samples of about 10 mm length. Then, each cylindrical gel sample was placed on a digital balance. A load was transmitted vertically to the gel through a rod fitted with a PTFE end-plate [21]. The force acting on the gel was calculated from the reading of the balance m as $F = mg$, where g is the gravitational acceleration. The resulting deformation $\Delta l = l_0 - l$, where l_0 and l are the initial undeformed and deformed lengths, respectively, was measured using a digital comparator (IDC type Digimatic Indicator 543-262, Mitutoyo Co.), which was sensitive to displacements of 10^{-3} mm. The force and the resulting deformation were recorded after 20 s of relaxation. The measurements were conducted up to about 20% compression. The deformation ratio α (deformed length/initial length) was calculated as $\alpha = 1 - \Delta l/l_0$. The corresponding stress f was calculated as $f = F/A$, where A is the cross-sectional area of the specimen, $A = \pi r_0^2$, where r_0 is its initial radius. The elastic modulus G_0 of gels just after their preparation was determined from the slope of linear dependence $f = G_0(\alpha - \alpha^{-2})$.

3. Results and discussion

We first monitored the formation of hydrogels with various hydrophobic group contents by real-time light scattering measurements. Fig. 1 shows the scattered light intensity I_s recorded at $\theta = 90°$ plotted as a function of reaction time in free-radical crosslinking copolymerization of AAm/DMA comonomer system with BAAm as the crosslinker. All the synthesis parameters were fixed in the experiments except that the composition of the comonomer mixture was varied. As expected, no intensity rise was observed during the induction period of the reactions. The start of the polymerization is accompanied with a rapid increase in I_s, which reaches a maximum after a short reaction time. As was shown before, the maximum in the scattering curve corresponds to the point at which the polymer concentration in the reaction system attains the critical overlap concentration c^* [20,22]. Gelation

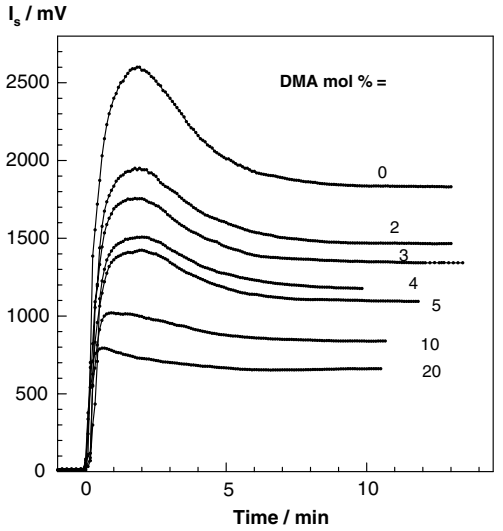

Fig. 1. The scattered light intensity I_s recorded at $\theta = 90°$ shown as a function of the reaction time for crosslinking AAm/DMA copolymerization at various DMA content, as indicated in the figure.

occurs at or beyond the maximum point of the scattering curves [20]. After passing the maximum intensity, I_s gradually decreases with the reaction time and finally, attains a plateau value after about 10 min. The decrease of I_s in long reaction times is due to the increase of the polymer concentration. Comparison of the scattering curves shows that the addition of DMA into the comonomer feed decreases the scattered light intensity. The higher the DMA content, the lower is the scattered light intensity. Further, the maxima of the scattering curves slightly shift toward short reaction times as the DMA content of the comonomer feed is increased.

In order to generalize the above findings, we measured the scattered light intensities from gels at various scattering angles. The reaction time for the hydrogel preparation was set to 24 h. Using the gravimetric technique [23], no unreacted monomer or soluble polymer was detected in the reaction systems after 24 h, indicating that the gel fraction was complete. Fig. 2a and b show the Rayleigh ratio $R(q)$ vs the scattering vector q plots for the hydrogels and for the corresponding copolymer solutions at various DMA contents, respectively. The copolymer solutions were prepared under the same reaction conditions as the hydrogels except that the crosslinker BAAm was not used. For both hydrogels and polymer solutions, the light scattering intensity does not change much with the scattering vector q. This is due to the fact that we are in the semidilute regime for polymer solutions and we are probing length scales large compared with those typical for polymer hydrogels. Therefore, we will focus on the scattering intensities measured at a fixed scattering angle $\theta = 90°$ which corresponds to the scattering vector $q = 1.7 \times 10^{-3}$ Å^{-1}. Another point shown in Fig. 2a and b is that the hydrogel scatters much more light than the corresponding polymer solution, especially at low DMA contents. The excess scattering from hydrogels over the scattering from polymer solution, $R_{ex,q}$, was calculated as

$$R_{ex,q} = R_{gel,q} - R_{sol,q} \quad (1)$$

where $R_{gel,q}$ and $R_{sol,q}$ are the Rayleigh ratios for gel and polymer solution at a fixed scattering vector q,

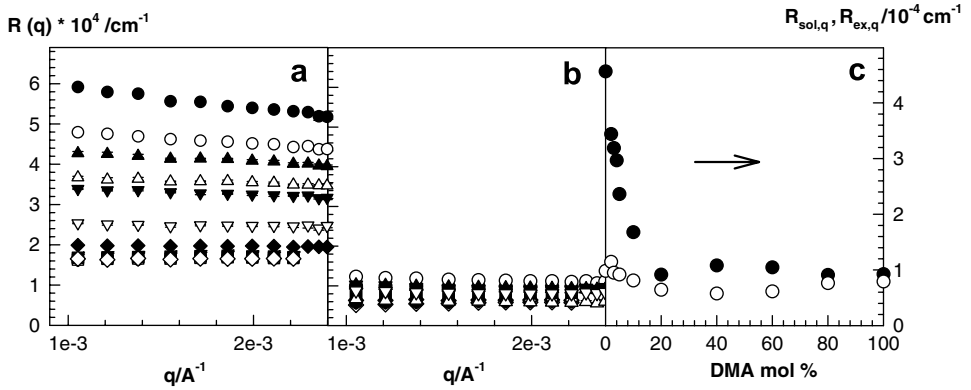

Fig. 2. (a), (b) Rayleigh ratio $R(q)$ versus scattering vector q plots for the AAm/DMA gels (a) and for the corresponding linear polymer solutions (b). DMA mol% = 0 (●), 2 (○), 3 (▲), 4 (△), 5 (▼), 10 (▽), 20 (◆), 40 (◇), 60 (⬢), 80 (□), and 100 (■). (c) The excess scattering $R_{ex,q}$ (filled symbols) and the scattering from solutions $R_{sol,q}$ (open symbols), measured at $q = 1.7 \times 10^{-3}$ Å^{-1} shown as a function of DMA mol%.

respectively. Since the thermal concentration fluctuations in hydrogels are eliminated in $R_{ex,q}$, excess scattering is a measure of the degree of spatial inhomogeneities. Fig. 2c shows the excess scattering $R_{ex,q}$ (filled symbols) and the scattering from solutions $R_{sol,q}$ (open symbols) plotted as a function of DMA concentration. The scattering intensity from polymer solution $R_{sol,q}$ slightly decreases with the DMA content. In contrast, however, the excess scattering $R_{ex,q}$ rapidly decreases up to 20 mol% DMA and then remains constant. The results demonstrate that the hydrogels become increasingly homogeneous with increasing amount of DMA up to 20 mol%.

Dynamics of the hydrogels were investigated by DLS measurements as a function of DMA content. DLS provides the time average intensity correlation function $g_T^{(2)}(q,\tau)$, defined as [24]

$$g_T^{(2)}(q,\tau) = \frac{\langle I(q,0)I(q,\tau)\rangle_T}{\langle I(q,0)\rangle_T^2} \quad (2)$$

whose short-time limit can be related to an apparent diffusion coefficient, D_A, via [24,25]

$$D_A = -\frac{1}{2q^2}\lim_{\tau\to 0}\ln(g_T^{(2)}(q,\tau)-1) \quad (3)$$

where τ is the decay time, and $\langle\cdots\rangle_T$ denotes time average. For a nonergodic medium like polymer gels, D_A and likewise, the time-averaged scattering intensity $\langle I(q)\rangle_T$ varies randomly with sample position. $\langle I(q)\rangle_T$ has two contributions, one from static inhomogeneities (frozen structure) and the other from dynamic fluctuations, which are represented by the following equation [24–26]:

$$\langle I(q)\rangle_T = I_C(q) + \langle I_F(q)\rangle_T \quad (4)$$

where $I_C(q)$ and $\langle I_F(q)\rangle_T$ are the scattered intensity due to the frozen structure and liquidlike concentration fluctuations, respectively. To separate $\langle I(q)\rangle_T$ into its two parts, we follow the method proposed by Joosten et al. [24]. Treating the system by the partial heterodyne approach, one obtains

$$D = D_A/(2-X) \quad (5)$$

where D is the cooperative diffusion coefficient and $X = \langle I_F(q)\rangle_T/\langle I(q)\rangle_T$. Eq. (5) applies to each sample position. For different sample positions, different values of D_A and $\langle I(q)\rangle_T$ are obtained. Then, if many measurements at different sample positions are performed, the cooperative diffusion coefficient D and the fluctuating component of the scattering intensity $\langle I_F(q)\rangle_T$ can be obtained by plotting $\langle I(q)\rangle_T/D_A$ vs $\langle I(q)\rangle_T$ according to Eq. (5a), which is simply a rearrangement of Eq. (5).

$$\frac{\langle I(q)\rangle_T}{D_A} = \frac{2\langle I(q)\rangle_T}{D} - \frac{\langle I_F(q)\rangle_T}{D} \quad (5a)$$

Fig. 3a–c show the variations of the time-averaged scattered intensity $\langle I\rangle_T$, measured at $\theta = 90°$, with the sample position for the hydrogels with 0, 5, and 50 mol% DMA, respectively. The solid lines indicate the ensemble-averaged scattered intensity, $\langle I\rangle_E$, obtained by averaging $\langle I\rangle_T$ with respect to sample position. The fluctuations in $\langle I\rangle_T$ decreases as the DMA content in the comonomer feed is increased. Thus, increasing amount of DMA suppresses the frozen concentration fluctuations in PAAm hydrogels. In order to extract the contribution of dynamic fluctuation component in the scattered intensity, decomposition of $\langle I\rangle_T$ was carried out by using Eq. (5a). Fig. 4 shows typical decomposition plots for three hydrogel samples with 0,

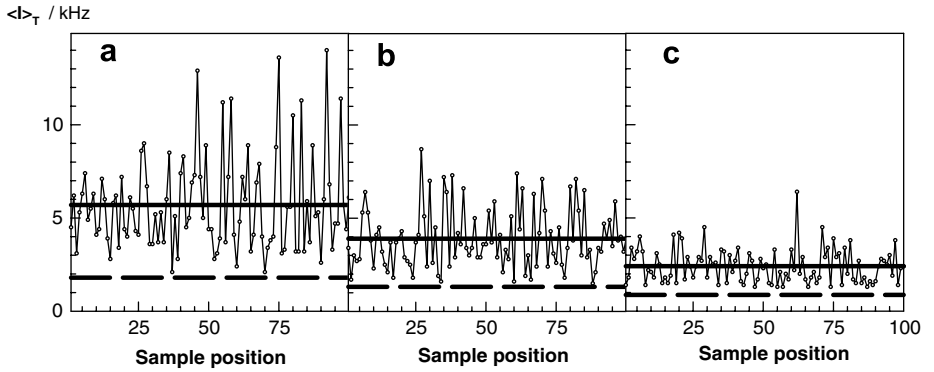

Fig. 3. Variation of the time-averaged scattered intensity $\langle I\rangle_T$ with the sample position for PAAm hydrogels with 0 (a), 5 (b), and 50 mol% DMA (c). The solid lines represent the ensemble-averaged scattered intensity $\langle I\rangle_E$. The fluctuating component of the scattered intensity $\langle I_F\rangle_T$ are represented by the dashed lines.

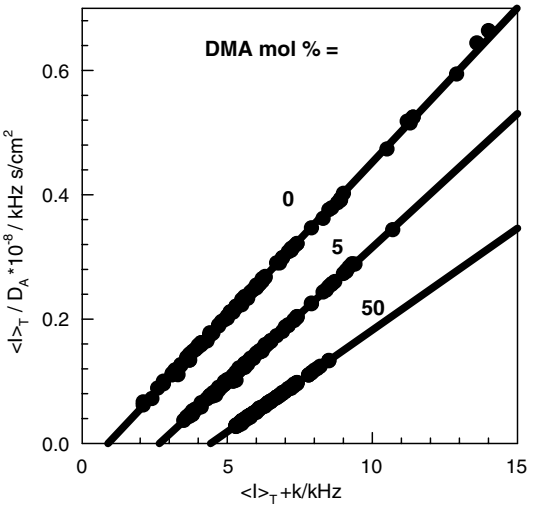

Fig. 4. Decomposition plots according to Eq. (5a) for hydrogels with DMA contents indicated in the figure. k is the shift factor taken as 0, 2, and 4 for gels with 0, 5, and 50 mol% DMA, respectively.

5, and 50 mol% DMA. For each system 100 data points are plotted. From the linear regression analysis of hydrogels with various DMA content, diffusion coefficients D as well as the fluctuating component of the scattered intensity $\langle I_F \rangle_T$ were evaluated. The dashed lines in Fig. 3 represent $\langle I_F \rangle_T$ values for gels with 0, 5, and 50 mol% DMA.

In Fig. 5a, the scattered intensities due to the frozen structure I_C and due to the liquidlike concentration fluctuations $\langle I_F \rangle_T$ are plotted against the DMA content. Both I_C and $\langle I_F \rangle_T$ decrease up to about 20 mol% DMA and then remain almost unchanged. The results are in good agreement with those obtained from static light scattering experiments (Fig. 2c). It should be pointed out that, in the treatment of the static light scattering data, the fluctuating component of the scattered intensity of gels is assumed to be equal to the scattered light intensity from the corresponding semidilute polymer solution, i.e., $\langle I_F \rangle_T = I_{sol}$. The agreement between static and dynamic light scattering results, as shown in Figs. 2c and 5a also demonstrate that, at least for the present gel systems, this is a reasonable approximation.

In Fig. 5b, the cooperative diffusion coefficient D and the dynamic correlation length ξ_{DLS} are plotted against DMA%. ξ_{DLS} was evaluated by [27]

$$\xi_{DLS} = \frac{kT}{6\pi\eta D} \tag{6}$$

where η is the viscosity of the medium (8.86×10^{-4} Pa s) and kT is the Boltzmann energy. The diffusion coefficient D is an increasing function so that

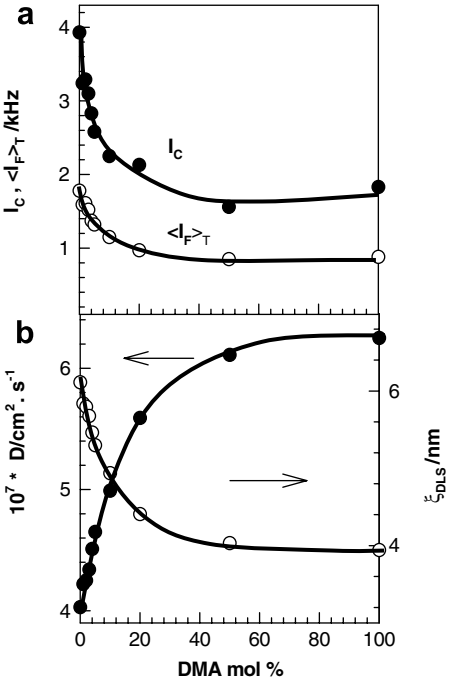

Fig. 5. (a) Variations of the scattered intensities due to the frozen structure I_C (filled circles) and due to the liquidlike concentration fluctuations $\langle I_F \rangle_T$ (open circles) plotted against DMA%. (b) The cooperative diffusion coefficient D (filled circles) and the dynamic correlation length ξ_{DLS} (open circles) plotted against DMA%.

the mesh size ξ_{DLS} is a decreasing function of DMA%. Since the crosslinker ratio, that is the mole ratio of the crosslinker BAAm to the monomers AAm + DMA was fixed in the preparation of the hydrogels, the decrease of the mesh size ξ_{DLS} suggests increasing crosslinking efficiency of BAAm as the DMA content is increased. This result may be attributed to the homogenization of hydrogels in the presence of DMA up to 20 mol%. As the crosslinks are distributed uniformly throughout the gel sample, the number of highly crosslinked zones decreases so that an increasing number of BAAm molecules are involved in the formation of effective crosslinks. This would lead to an increase in the effective crosslink density and to a decrease in the mesh size of the hydrogels.

In order to check the DLS results regarding the variation of the mesh size of the hydrogels depending on the DMA content, elasticity measurements were carried out. In Fig. 6, the filled circles represent the moduli of elasticity G_0 of hydrogels just after their preparation plotted against DMA mol%. The average molecular weight between crosslinking points, $\overline{M}_c$, is related to the elastic modulus G_0 through the equation [28,29]

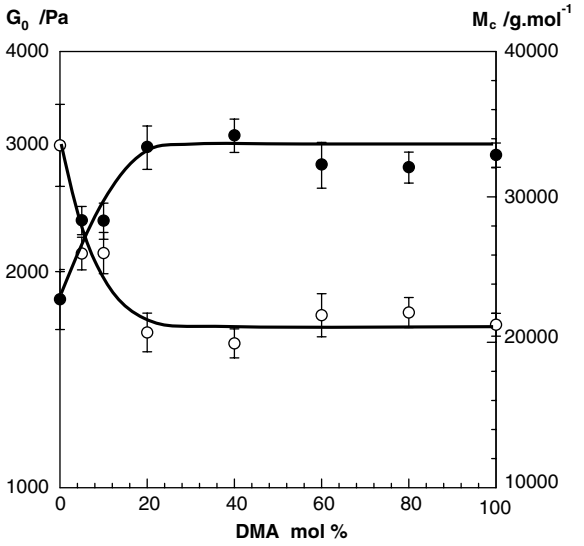

Fig. 6. The modulus of elasticity G_0 of hydrogels after preparation (filled circles) and the average molecular weight between crosslinking points $\overline{M}_c$ plotted against DMA mol%.

$$\overline{M}_c = A\rho RT v_2^0/G_0 \tag{7}$$

where the front factor A equals to 1 for an affine network, and $1–2/\phi$ for a phantom network, ϕ is the functionality of the crosslinks, ρ is the polymer density, R is the gas constant, and v_2^0 is the crosslinked polymer concentration after gel preparation. Assuming phantom network behavior ($\phi = 4$) and a polymer density $\rho = 1.35$ g/ml [30], the molecular weight $\overline{M}_c$ characterizing the average size of the network chains was calculated. The open circles in Fig. 6 show $\overline{M}_c$ of the hydrogels as a function of DMA mol%. In accord with the variation of the dynamic correlation length ξ_{DLS}, the network chain length decreases with increasing DMA% up to about 20 mol%.

The results thus show the homogenization effect of DMA in the preparation of PAAm hydrogels. We repeated the static light scattering measurements by replacing DMA with another hydrophobically modified hydrophilic monomer, namely, with the NIPA monomer. In contrast to DMA, NIPA is known to produce temperature sensitive hydrogels with a lower critical solution temperature of about 34 °C [31]. Even below this temperature, formation of heterogeneous PNIPA hydrogels was reported due to the exothermicity of the polymerization reactions [32]. Therefore, we limited the NIPA content of the comonomer mixture with 20%. Fig. 7a and b show the Rayleigh ratio $R(q)$ vs the scattering vector q plots for the hydrogels and for the corresponding AAm/NIPA copolymer solutions at various NIPA contents, respectively. Fig. 7c shows the excess scattering $R_{ex,q}$ (filled symbols) and the scattering from solutions $R_{sol,q}$ (open symbols) plotted as a function of NIPA concentration. The scattering intensity from polymer solution $R_{sol,q}$ slightly decreases while the excess scattering $R_{ex,q}$ rapidly decreases with increasing amount of NIPA in the comonomer feed. Thus, the addition of NIPA as a comonomer also homogenizes PAAm hydrogels.

To interpret static light scattering results from gels, several functional forms of excess scattering $R_{ex}(q)$ have been proposed empirically, i.e., Debye–Bueche, Guinier, and Ornstein–Zernicke functions [33–41]. For example, according to the Debye–Bueche function, $R_{ex}(q)$ is given by [33–36]

$$R_{ex}(q) = \frac{4\pi K \xi^3 \langle \eta^2 \rangle}{(1+q^2\xi^2)^2} \tag{8}$$

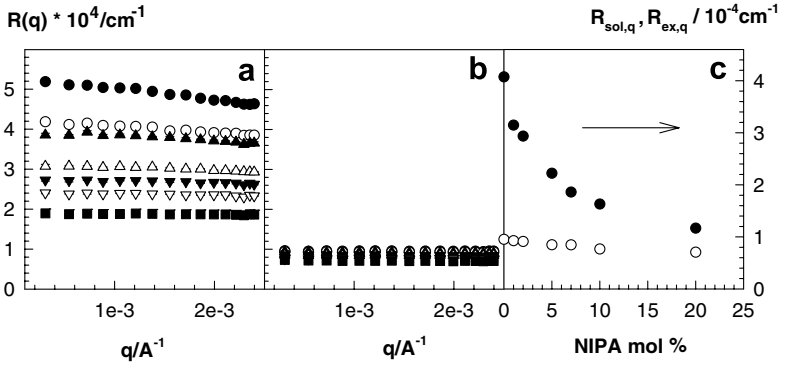

Fig. 7. (a), (b) Rayleigh ratio $R(q)$ versus scattering vector q plots for the AAm/NIPA gels (a) and for the corresponding linear polymer solutions (b). NIPA mol% = 0 (●), 1 (○), 2 (▲), 5 (△), 7 (▼), 10 (▽), and 20 (■). (c) The excess scattering $R_{ex,q}$ (filled symbols) and the scattering from solutions $R_{sol,q}$ (open symbols), measured at $q = 1.7 \times 10^{-3}$ Å^{-1} shown as a function of NIPA mol%.

where K being the optical constant, $K = 8\pi^2 n^2 \lambda^{-4}$, ξ is the static correlation length of the scatterers, and $\langle \eta^2 \rangle$ is the mean square fluctuation of the refractive index. According to Eq. (8), the slope and the intercept of $R_{ex}(q)^{-1/2}$ vs q^2 plot (Debye–Bueche plot) give ξ and $\langle \eta^2 \rangle$ of a gel sample. In Fig. 8, the excess scattering data from AAm/NIPA copolymer hydrogel samples are given in the form of Debye-plots. Straight lines are obtained in this analysis, indicating that the Debye–Bueche function works well. Such straight lines were also obtained for AAm/DMA hydrogels. Calculated values of ξ and $\langle \eta^2 \rangle$ from the Debye–Bueche analysis are shown in Fig. 9a and b, respectively, plotted as a function of NIPA or DMA%. The filled and open circles are data points obtained from hydrogels containing NIPA and DMA segments, respectively. ξ decreases while $\langle \eta^2 \rangle$ increases as the DMA or NIPA concentration is increased. In Fig. 9a, the dynamic correlation lengths ξ_{DLS} of AAm/DMA hydrogels obtained from DLS measurements are also shown by the open triangles. It is seen that, both ξ and ξ_{DLS} are at the same order of magnitude and show similar DMA% dependence. This indicates that the static correlation length calculated from Debye–Bueche analysis corresponds to the dynamic correlation length of DLS results.

One may speculate about the cause of the homogenization occurring in the hydrogels that contain DMA or NIPA segments. As reported before, free-radical polymerization of DMA produces much higher molecular weight polymers compared to the

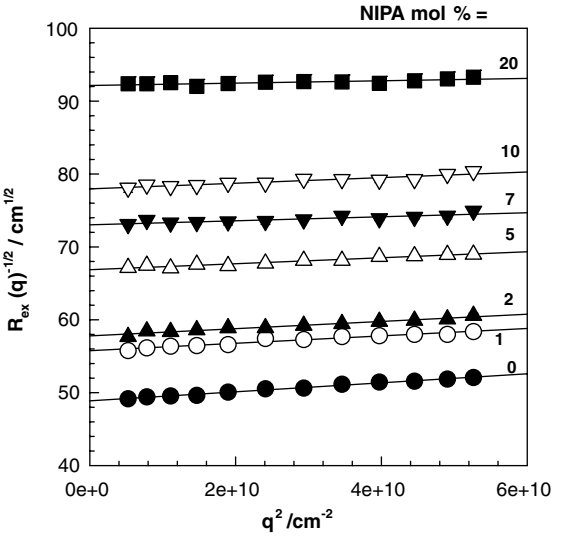

Fig. 8. Debye–Bueche plots for PAAm gels prepared at various NIPA mol% indicated in the figure.

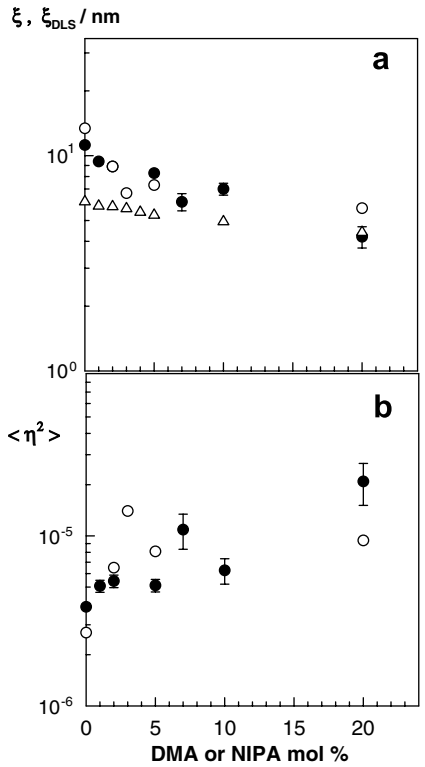

Fig. 9. (a) The dynamic correlation length ξ_{DLS} of AAm/DMA hydrogels obtained from DLS measurements (open triangles) and the static correlation length ξ calculated from the Debye–Bueche analysis (circles) shown as a function of DMA or NIPA%. The filled and open circles are the ξ data obtained from hydrogels containing NIPA and DMA segments, respectively. (b) The mean square fluctuation of the refractive index $\langle \eta^2 \rangle$ in hydrogels shown as a function of DMA or NIPA%. The filled and open circles are data points obtained from hydrogels containing NIPA and DMA segments, respectively.

AAm polymerization [20]. It was also shown that, the higher the DMA content of the comonomer feed in linear DMA/AAm copolymerization, the higher the molecular weight of the polymer [42]. This is due to the steric effect of alkyl side groups of PDMA chains, which reduce the rate of termination reactions. The shift of the maxima in the scattering curves toward short reaction times also indicates earlier onset of the critical overlap (c^*) concentration due to the formation of larger polymer coils in the presence of DMA (Fig. 1). Similar to the termination reactions, crosslinking reactions also occur between two polymer molecules. Thus, one may expect a reduction in the rate of crosslinking reactions on rising the DMA content, which would shift the gelation threshold to later reaction times. Indeed, it was shown that gelation in the crosslinking AAm polymerization occurs around the c^* concentration, while

in the crosslinking DMA polymerization, it occurs in the semidilute regime of the reaction system [20]. Thus, as the DMA content is increased, solution of linear and branched polymers crosses the semidilute regime prior to the onset of gelation. Since crosss-links are introduced relatively randomly in space during crosslinking of preformed polymer chains, increasing content of DMA in the comonomer feed decreases the degree of spatial gel inhomogeneity of PAAm hydrogels. Previous work shows that both poly(DMA) and poly(NIPA) hydrogels are much more homogeneous than the corresponding PAAm gels [20,43]. These findings are in accord with our observations.

4. Conclusions

Network microstructures of acrylamide (AAm)-based hydrogels were investigated by static and dynamic light scattering techniques. It was observed that the addition of hydrophobically modified hydrophilic monomers, such as DMA or NIPA, into the comonomer feed decreases the excess scattering $R_{ex,q}$, indicating that the hydrogels become increasingly homogeneous with increasing amount of DMA or NIPA. In accord with the static light scattering results, DLS also shows suppression of the frozen concentration fluctuations in PAAm hydrogels as the hydrophobic group content is increased. The cooperative diffusion coefficient increases while both the static and dynamic correlation lengths decrease as the amount of DMA in the comonomer feed is increased. Increasing degree of structural homogeneity of PAAm hydrogels with increasing hydrophobic group content can be explained as a result of the steric effect of the bulky side groups on DMA or NIPA segments.

Acknowledgements

Work was supported by the Scientific and Technical Research Council of Turkey (TUBITAK), TBAG –105T246. O. Okay is very grateful to Alexander von Humboldt Stiftung for a grant.

References

[1] Funke W, Okay O, Joos-Muller B. Adv Polym Sci 1998;136:139.
[2] Okay O. Prog Polym Sci 2000;25:711.
[3] Bastide J, Candau SJ. In: Cohen Addad JP, editor. Physical properties of polymeric gels. Wiley; 1996. p. 143.
[4] Shibayama M. Macromol Chem Phys 1998;199:1.
[5] Mallam S, Horkay F, Hecht AM, Geissler E. Macromolecules 1989;22:3356.
[6] Ikkai F, Shibayama M. Phys Rev E 1997;56:R51.
[7] Cohen Y, Ramon O, Kopelman IJ, Mizraki S. J Polym Sci Polym Phys Ed 1992;30:1055.
[8] Schosseler F, Skouri R, Munch JP, Candau SJ. J Phys II 1994;4:1221.
[9] Shibayama M, Tanaka T, Han CC. J Chem Phys 1992; 97:6842.
[10] Horkay F, McKenna GB, Deschamps P, Geissler E. Macromolecules 2000;33:5215.
[11] Moussaid A, Candau SJ, Joosten JGH. Macromolecules 1994;27:2102.
[12] Skouri R, Schosseler F, Munch JP, Candau SJ. Macromolecules 1995;28:197.
[13] Kizilay MY, Okay O. Polymer 2003;44:5239.
[14] Yazici I, Okay O. Polymer 2005;46:2595.
[15] Ikkai F, Shibayama M. J Polym Sci Part B Polym Phys 2005;43:617.
[16] Hecht AM, Duplessix R, Geissler E. Macromolecules 1985;18:2167.
[17] Shibayama M, Ikkai F, Nomura S. Macromolecules 1994;27:6383.
[18] Cerid H, Okay O. Eur Polym J 2004;40:579.
[19] Kizilay MY, Okay O. Macromolecules 2003;36:6856.
[20] Orakdogen N, Kizilay MY, Okay O. Polymer 2005; 46:11407.
[21] Sayil C, Okay O. Polymer 2001;42:7639.
[22] Orakdogen N, Okay O. J Appl Polym Sci 2007;103:3228.
[23] Durmaz S, Okay O. Polymer 2000;41:3693.
[24] Joosten JGH, McCarthy JL, Pusey PN. Macromolecules 1991;24:6690.
[25] Pusey PN, van Megen W. Physica A 1989;157:705.
[26] Ikkai F, Shibayama M. Phys Rev Lett 1999;82:4946.
[27] De Gennes PG. Scaling concepts in polymer physics. Ithaca, NY: Cornell University Press; 1979.
[28] Flory PJ. Principles of polymer chemistry. Ithaca, NY: Cornell University Press; 1953.
[29] Treloar LRG. The physics of rubber elasticity. Oxford: University Press; 1975.
[30] Ilavsky M. Macromolecules 1982;15:782.
[31] Hirokawa Y, Tanaka T. J Chem Phys 1984;81:6379.
[32] Kara S, Okay O, Pekcan O. J Appl Polym Sci 2002;86: 3589.
[33] Bueche F. J Colloid Interface 1970;33:61.
[34] Debye PJ. J Chem Phys 1959;31:680.
[35] Debye P, Bueche AM. J Appl Phys 1949;20:518.
[36] Soni VK, Stein RS. Macromolecules 1990;23:5257.
[37] Horkay F, Hecht AM, Geissler E. Macromolecules 1994;27:1795.
[38] Shibayama M, Tanaka T, Han CC. J Chem Phys 1992;97: 6829.
[39] Wu W, Shibayama M, Roy S, Kurokawa H, Coyne LD, Nomura S, et al. Macromolecules 1990;23:2245.
[40] Higgins JS, Benoit HC. Polymers and neutron scattering. Oxford: Clarendon Press; 1994.
[41] Baumgaertner A, Picot CE. Molecular basis of polymer networks. Berlin: Springer-Verlag; 1989.
[42] Hocking MB, Klimchuk KA, Lowen S. J Polym Sci Part A Polym Chem 2000;38:3128.
[43] Takata S, Norisuye T, Shibayama M. Macromolecules 1999;32:3989.